U.S.NRC
United States Nuclear Regulatory Commission
Protecting People and the Environment

Technical Letter Report
TLR-RES/DE/REB-2021-13
Enclosure 2

Assessment of Reactor Pressure Vessel Inside Diameter Shallow Surface Breaking Flaws Second Progress Report: July 2019

Date:

December 2021

Prepared in response to Task 2 in User Need Request NRR-2017-007, by:

Marvin Smith
NUMARK Associates, Inc.

Terry Dickson
NUMARK Associates, Inc.

Andrew Dyszel
NUMARK Associates, Inc.

NRC Project Manager:

Patrick Raynaud
Senior Materials Engineer
Component Integrity Branch

Division of Engineering
Office of Nuclear Regulatory Research
U.S. Nuclear Regulatory Commission
Washington, DC 20555–0001

DISCLAIMER

This report does not contain or imply legally binding requirements. Nor does this report establish or modify any regulatory guidance or positions of the U.S. Nuclear Regulatory Commission and is not binding on the Commission.

NUMARK ASSOCIATES, INC.

Assessment of Reactor Pressure Vessel Inside Diameter Shallow Surface Breaking Flaws
Second Progress Report: July 2019

Prepared For:
U.S. Nuclear Regulatory Commission
Washington, DC

NRC Project Manager and Technical Director:
Patrick Raynaud
NRC/RES/DE/CIB

Prepared by:
Marvin Smith, Terry Dickson, Andrew Dyszel
NUMARK ASSOCIATES INC.

July, 2019

NUMARK ASSOCIATES, INC.

Table of Contents

NUMARK ASSOCIATES, INC.

List of Figures

List of Tables

Acronyms

ASME	American Society of Mechanical Engineers
BWR	Boiling Water Reactor
CPF	Conditional Probability of vessel Failure. The probability is termed conditional because it assumes that the analyzed transient has occurred. To transform CPF into a risk metric it must be multiplied by the probability of the transient occurring.
CPI	Conditional Probability of crack Initiation. The probability is termed conditional because it assumes that the analyzed transient has occurred. To transform CPI into a risk metric it must be multiplied by the probability of the transient occurring.
CTE	Coefficient of Thermal Expansion
EFPY	Effective Full-Power Years
EPFM	Elastic-Plastic Fracture Mechanics
FAVOR	Fracture Analysis of Vessels – Oak Ridge
FEM	Finite-Element Method
ID	Inner Diameter
LEFM	Linear-Elastic Fracture Mechanics
NPP	Nuclear Power Plants
NRC	United States Nuclear Regulatory Commission
ORNL	Oak Ridge National Laboratory
PFM	Probabilistic Fracture Mechanics
PNNL	Pacific Northwest National Laboratory
P-T	Pressure and Temperature Limits
PTS	Pressurized Thermal Shock
PWR	Pressurized Water Reactor
RCS	Reactor Coolant System
RPV	Reactor Pressure Vessel
SFT	Stress-Free Temperature
SIFIC	Stress-intensity Factor Influence Coefficients
TWCF	Through-Wall Cracking Frequency; which is calculated as a product of the CPF and a matrix defining the sequence (or event) frequency of the loading transients. Calculating a mean TWCF for RPVs subjected to pressure and temperature curves requires a statistical representation of the possible transients and their frequencies of occurrence.
WPS	Warm Pre-Stress

1 Introduction

1.1 Background

As a follow-up to the 2016 ORNL Report on "The Effect of Shallow Inside-Surface-Breaking Flaws on the Probability of Brittle Fracture of Reactors Subjected to Postulated and Actual Operational Cool-Down Transients: A Status Report" (Reference (1) – hereafter referred to as ORNL 2016), additonal literature searches and sensitivity studies were performed and discussed in an "Assessment of Reactor Pressure Vessel Inside Diameter Shallow Surface Breaking Flaws," Reference (2) – hereafter referred to as NUMARK 2018. The Fracture Analysis of Vessels – Oak Ridge (FAVOR -Reference (3)) Version 16.1 Probabilistic Fracture Mechanics (PFM) computer code was used to perform these additional sensitivity analyses to further examine the impact of shallow surface breaking flaws on Reactor Pressure Vessel (RPV) structural integrity.

FAVOR analyses of shallow internal surface-breaking flaws presented in ORNL 2016 found that normal cooldown transients may result in Conditional Probability of Crack Initiation (CPI) and Conditional Probability of Vessel Failure (CPF) above 10^{-6}. Because plant cooldown transients are normal plant operations that occur with a frequency of at least once per refueling cycle, the annual TWCF for these shallow flaws may also exceed 10^{-6}.

Studies reported in NUMARK 2018 were performed to determine whether more realistic assumptions for stress-free temperature, warm pre-stress or other analysis assumptions could be identified that would reduce the estimated annual TWCF to below 10^{-6}. Because the analyses presented in NUMARK 2018 did not identify changes in analyses assumptions to achieve a reduction in TWCF to less than 10^{-6}, additional studies were recommended including evaluations of shallow flaws based on actual plant cooldown pressure-temperature time histories.

This current report extends the work reported in NUMARK 2018 and documents analyses of shallow flaws based on eleven actual plant cooldowns for four plants (referred to as PWR A, PWR B, PWR C, and PWR D) with a range of clad thickness and reactor vessel embrittlement.

1.2 Objective and Report Outline

The objective of this report is to evaluate shallow surface breaking flaws based on plant cooldown at the maximum rate allowed by typical plant P-T limit curves (100°F per hour), and compare the resulting calculated TWCF to plant cooldowns based on actual recorded plant pressure-temperature cooldown profiles. The Fracture Analysis of Vessels – Oak Ridge (FAVOR -Reference (3)) Version 16.1 Probabilistic Fracture Mechanics (PFM) computer code was used to evaluate these plant cooldowns and to examine the impact of postulated shallow surface breaking flaws on Reactor Pressure Vessel (RPV) structural integrity.

In addition to evaluating plant cooldowns for the Palisades plant used for ORNL 2016 and NUMARK 2018 studies (hereafter referred to as PWR A), three additional plants with diverse are evaluated, referred to as PWR B, PWR C, and PWR D. The shallow flaw analyses presented in this report assume one surface breaking flaw in the reactor pressure vessel. The reactor vessel beltline region is modeled based on the active fuel height plus 12 inches above and below this height. Because these inside surface breaking

flaws originate in the clad that is uniformly applied over the entire pressure vessel inside surface, the probability of occurrence for the single flaw is assumed to be uniform across this beltline surface area. The distribution of flaw aspect ratio assumed is the same as used in previous shallow flaw studies (Reference (1)): 67.45% aspect ratio of 2, 20.77% aspect ratio of 6, 3.96% aspect ratio of 10 and 7.82% aspect ratio of infinity.

Based on the studies presented in ORNL 2016 and NUMARK 2018, the limiting flaw depth that produces the highest Conditional Probability of Crack Initiation (CPI) and Conditional Probability of RPV Failure (CPF) is a flaw that extends just through the clad into the ferritic steel.

Because the FAVOR code limits flaw depth to 1% increments of RPV wall thickness, the flaw depth is chosen for each vessel as the minimum 1% increment that just extends through the stainless steel clad into the ferritic steel vessel wall. The clad thickness and flaw depth for the four plants evaluated are shown in Table 1. An evaluation of CPI as a function of flaw depth is provided in Appendix A. As shown in Appendix A, the CPI for shallow flaws is generally a maximum for the 1% increment flaw depth that extends just beyond the clad thickness. The CPI at the next increment may be approximately equal to this first value and then CPI generally drops by several orders of magnitude at flaw depths further from the clad. In addition to evaluations of these shallow flaws, each vessel was also evaluated for the ¼ thickness flaw that is normally assumed per ASME Appendix G (4).

Table 1 – Clad Thickness and Flaw Depths Evaluated

Plant	Vessel Wall Thickness (in.)	Clad Thickness (in.)	Clad Thickness (% wall)	Flaw Depth (% of RPV Wall)	Flaw Depth (in.)	Depth into Ferritic (in.)
PWR A	8.750	0.250	2.86%	3%	0.2625	0.0125
PWR A	8.750	0.250	2.86%	4%	0.3500	0.1000
PWR A	8.750	0.250	2.86%	5%	0.4375	0.1875
PWR B	8.988	0.313	3.48%	4%	0.3595	0.0465
PWR C	8.626	0.188	2.18%	3%	0.2588	0.0708
PWR D	8.036	0.156	1.94%	2%	0.1607	0.0047

These four plants are evaluated for a 100°F per hour constant cooldown and for the 11 actual plant cooldown pressure-temperature profiles selected for this study. Based on the results of these actual plant cooldowns, a simplified cooldown profile is developed that results in a calculated CPI/CPF that is conservative compared with these actual cooldown profiles. This simplified cooldown profile is then used to evaluate FAVOR code input assumptions including stainless-steel Coefficient of Thermal Expansion (CTE).

2 Impact of Plant Cooldown Transient on Shallow Flaw CPI/CPF

2.1 Maximum Allowable 100°F per hour Cooldown

The maximum cooldown rate allowed according to the ASME Boiler and Pressure Vessel Code, Section XI, Appendix G ASME (4) is 100°F per hour. In order to have a consistent evaluation to show the impact of vessel geometry, clad thickness and plant embrittlement on CPI/CPF, each of these four plants are evaluated for a 100°F per hour cooldown from 550°F to 70°F (288-minute cooldown time). The RCS pressure was decreased linearly from 2.25 ksi to 0.4 ksi over this same 288-minute cooldown time. This simultaneous pressure-temperature cooldown was selected as the base case for this study both because cooldown at the maximum pressure allowed by ASME Section XI Appendix G (4) may overestimate the effects of warm pre-stress and because plants generally reduce pressure along with temperature during plant cooldowns.

In addition to evaluating the shallow flaws listed in Table 1, each of the four plants were evaluated for the ¼ thickness flaw specified in ASME Section XI Appendix G (4) as the assumed maximum flaw depth for surface breaking flaws. ASME Section XI Appendix G implies that this ¼ thickness flaw would be limiting flaw for reactor vessel analysis. However, as shown below and as previously discussed in ORNL 2016, the ¼ thickness flaw may be protected against failure by warm pre-stress before the cooldown temperature approaches the lower shelf for K_{Ic} and may have a lower CPI/CPF than a shallow flaw.

The pressure-temperature profile for the 100°F per hour cooldown is shown in shown in Figure 1.

Figure 1 – 100°F per Hour Cooldown Pressure-Temperature Profile

The applied stress intensity K_I at the tip of a ¼ thickness (25%) flaw for PWR A with flaw aspect ratios of six and infinity are shown in Figure 2 along with K_{Ic} and aK_{IC} based on PWR A plant embrittlement. As shown in Figure 2, the peak applied stress intensity is reached before the applied stress exceeds either aK_{Ic} or KI_c. Therefore, crack initiation and vessel failure are prevented by warm pre-stress of the ¼ thickness flaw.

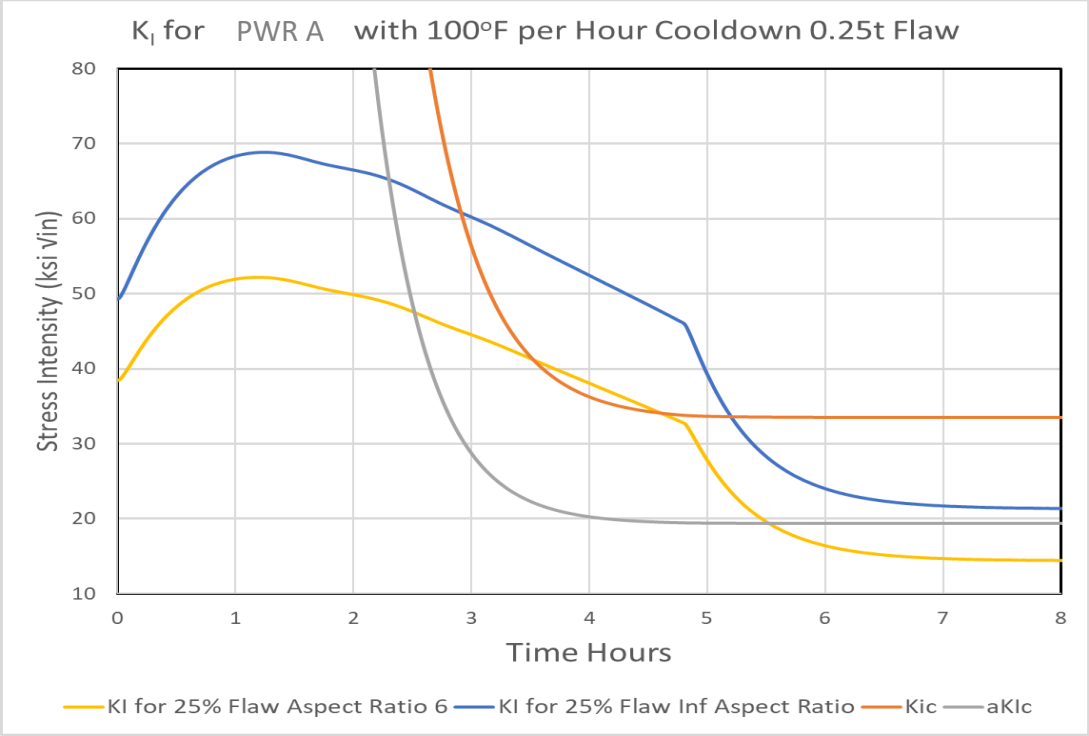

Figure 2 – PWR A K_I for 100°F per Hour Cooldown with ¼ t Flaw

The FAVOR code was used to calculate the CPI and CPF for the 100°F per hour cooldown shown in Figure 1 and the results of these analyses are shown in Table 2. As a result of warm pre-stress, the CPI and CPF are zero for all four plants.

Table 2 – CPI and CPF for ¼ Thickness Flaw and 100°F per Hour cooldown

Plant Geometry	RT_{PTS} at vessel ID	Cooldown Profile	Flaw Depth	CPI_{mean}	CPF_{mean}
PWR A	~ 320°F	100°F per hour	25%	0.00E+00	0.00E+00
PWR B	~ 300°F	100°F per hour	25%	0.00E+00	0.00E+00
PWR C	~ 260°F	100°F per hour	25%	0.00E+00	0.00E+00
PWR D	~ 275°F	100°F per hour	25%	0.00E+00	0.00E+00

To illustrate the importance of warm pre-stress, the FAVOR code was used to calculate the CPI and CPF for the 100°F per hour cooldown shown in Figure 1 without warm pre-stress, and the results of these analyses are shown in Table 3. Without consideration of warm pre-stress, the CPI and CPF for all four plants is well above 10^{-6}.

Table 3 – CPI and CPF for ¼ Thickness Flaw and 100°F per Hour Cooldown (no Warm Pre-stress)

Plant Geometry	RTPTS at vessel ID	Cooldown Profile	Flaw Depth	CPI $_{mean}$	CPF $_{mean}$
PWR A	~ 320°F	100°F per hour	25%	1.88E-03	1.70E-03
PWR B	~ 300°F	100°F per hour	25%	2.53E-04	1.16E-04
PWR C	~ 260°F	100°F per hour	25%	4.99E-05	2.36E-05
PWR D	~ 275°F	100°F per hour	25%	2.02E-04	1.73E-04

The applied stress intensity K_I at the tip for a shallow 3% flaw for PWR A with flaw aspect ratios of six and infinity is shown in Figure 3 along with K_{Ic} and aK_{IC} based on PWR A (60 EFPY) embrittlement. The applied stress intensity K_I at the tip for a shallow 4% flaw for PWR B with flaw aspect ratios of six and infinity is shown in Figure 4 along with K_{Ic} and aK_{IC} based on PWR B plant (60 EFPY) embrittlement.

As shown in Figure 3 and Figure 4, the peak applied stress intensity is reached after the applied stress exceeds aK_{Ic} or KI_c. Therefore, crack initiation and propagation are not prevented by warm pre-stress.

Figure 3 – PWR A K_I for 100°F Hour Cooldown with 3% Flaw

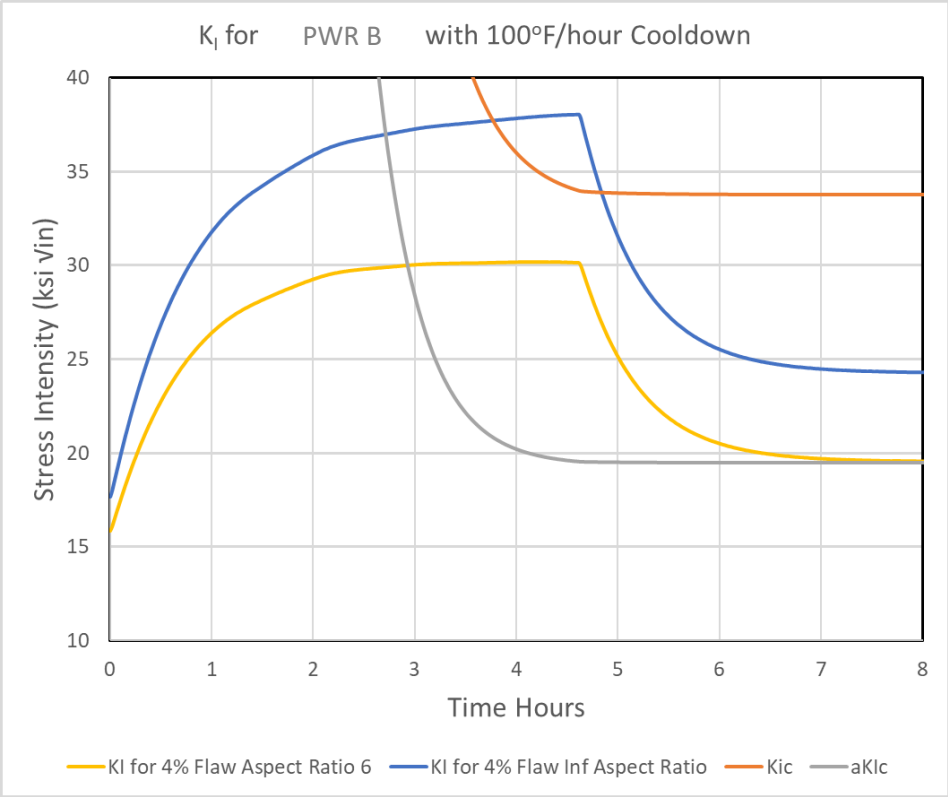

Figure 4 – PWR B K_I for 100°F per Hour Cooldown with 4% Flaw

The FAVOR code was used to calculate CPI and CPF for the Table 1 flaws and to determine the Through Wall Cracking Frequency assuming one plant cooldown per year. The results of these analyses are shown in Table 4. The calculated TWCF varies from 3.16 x 10^{-4} for the highest embrittlement plant (PWR A) to 1.35 x 10^{-6} for the lowest embrittlement plant (PWR D at 60 EFPY). In each case, the shallow flaw CPI and CPF is less than the CPI and CPF for the ¼ thickness flaw without warm pre-stress.

Table 4 – Evaluation of Shallow Flaws for 100°F per Hour Cooldown

Plant Geometry	Flaw Depth	CPI $_{mean}$	CPF $_{mean}$	Transients per year	Crack Initiation per year	TWCF
PWR A	3%	3.93E-04	3.16E-04	1.00E+00	3.93E-04	3.16E-04
PWR B	4%	7.67E-05	3.34E-06	1.00E+00	7.67E-05	3.34E-06
PWR C	3%	8.40E-06	2.26E-06	1.00E+00	8.40E-06	2.26E-06
PWR D	2%	4.19E-06	1.35E-06	1.00E+00	4.19E-06	1.35E-06

2.2 Actual Plant Cooldown Transients

Actual plant cooldowns were obtained from eleven different US PWR plants and one representative cooldown was selected for each of these plants. Figure 5 shows 10 actual cooldowns consistent with a cooldown before a refueling outage. As can be seen Figure 5, cooldown from operating temperature for refueling tends to occur at an initially high rate close to the ASME Section XI Appendix G specified maximum rate of 100°F per hour. This initial cooldown removes heat with the plant condenser system which is capable of rapid cooldown at a rate well above the ASME Section XI, Appendix G maximum 100°F per hour rate. After the RCS temperature cools down to approximately 300°F, the plant will shift over cooldown with the plant Residual Heat Removal (RHR) system. Based on the profiles for the 10 plant cooldown transients shown in Figure 5, cooldown after switchover to RHR tends to be at a lower rate than the cooldown to 300°F.

The Plant 7-1997 transient is not included in Figure 5 because the Plant 7-1997 transient included an extended time at full system pressure followed by a cooldown to near ambient temperature. The Plant 7-1997 transient was not a typical cooldown before a refueling outage. This transient was included in this actual cooldown analysis because it represents a different type of actual cooldown.

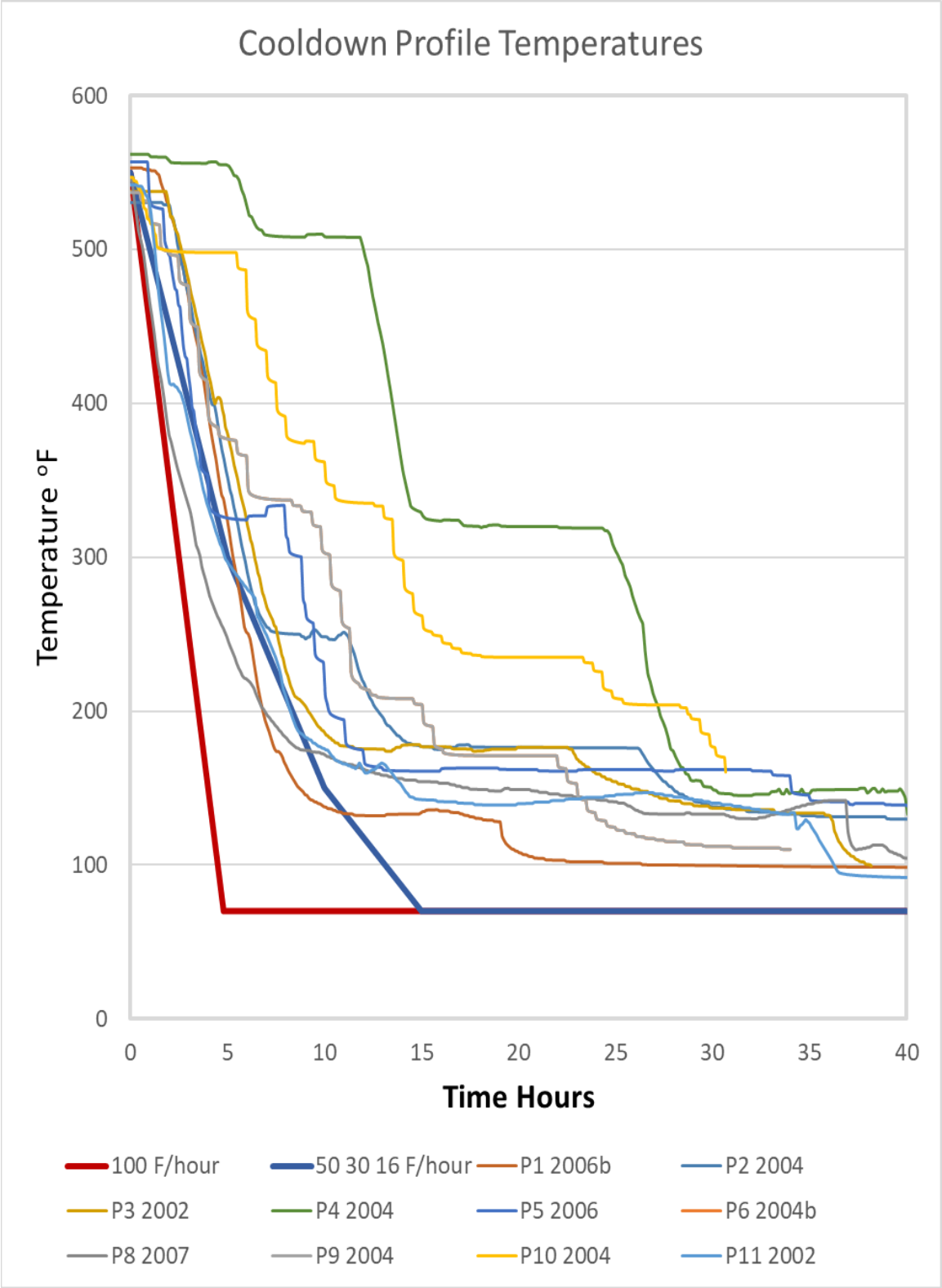

Figure 5 – Actual Plant Cooldown Temperature Profiles

The FAVOR code was used to analyze one 3% surface breaking flaw per vessel for these 11 actual plant P-T transients based on the plant geometry for PWR A with embrittlement based on RVID2 and other

available information. Table 5 shows the results of these actual plant cooldowns along with TWFC calculated assuming one transient per year. As shown in this table, the TWCF for these actual plant transients is substantially less than 10^{-6} for all 11 transients. The TWCF for the other three plants (PWR B, PWR C and PWR D) are lower than PWR A primarily because the embrittlement is lower for these other plants.

Table 5 – Actual Plant Cooldowns with PWR A Geometry, Embrittlement and 3% Flaw

Actual Cooldown	CPI $_{mean}$	CPF $_{mean}$	Transients per year	Crack Initiation per year	TWFC
Plant 1 2006b	1.22E-07	6.80E-16	1.00E+00	1.22E-07	6.80E-16
Plant 2 2004	8.40E-07	1.91E-12	1.00E+00	8.40E-07	1.91E-12
Plant 3 2002	6.49E-07	2.50E-13	1.00E+00	6.49E-07	2.50E-13
Plant 4 2004	5.60E-08	0.00E+00	1.00E+00	5.60E-08	0.00E+00
Plant 5 2004	1.42E-07	9.29E-13	1.00E+00	1.42E-07	9.29E-13
Plant 6 2004	2.37E-08	0.00E+00	1.00E+00	2.37E-08	0.00E+00
Plant 7 1997	2.05E-06	2.69E-10	1.00E+00	2.05E-06	2.69E-10
Plant 8 2007	2.35E-06	1.50E-08	1.00E+00	2.35E-06	1.50E-08
Plant 9 2004	1.40E-07	1.10E-11	1.00E+00	1.40E-07	1.10E-11
Plant 10 2004	9.77E-08	0.00E+00	1.00E+00	9.77E-08	0.00E+00
Plant 11 2002	1.74E-08	0.00E+00	1.00E+00	1.74E-08	0.00E+00

The actual plant transients with the highest CPI/CPF and TWCF are Plant 7-1997 and Plant 8-2007. The Plant 8-2007 cooldown transient appears to be a cooldown prior to a refueling outage. As shown in Figure 6, during the Plant 8 -2007 cooldown, the RCS temperature is reduced from 547°F to about 300°F in 3.6 hours at a rate of 69°F per hour. The cooldown from 300°F to 150°F occurs over the next 13.8 hours at an average of 11°F per hour. The initial pressure reduction from operating pressure of 2250 psia to 350 psia occurs over 2.7 hours. The pressure then remains at about 350 psia until about 38 hours when the RCS pressure is reduced to atmospheric to allow vessel head removal. At 37 hours after the cooldown begins, there is a 15-minute time period when the RCS temperature is reduced from 140°F to 115°F in at a rate of about 114°F per hour. The Plant 7-1997 and Plant 8-2007 transients produce the highest CPF of the 11 transients evaluated. However, assuming one transient per year, the TWCF is still well below 10^{-6}.

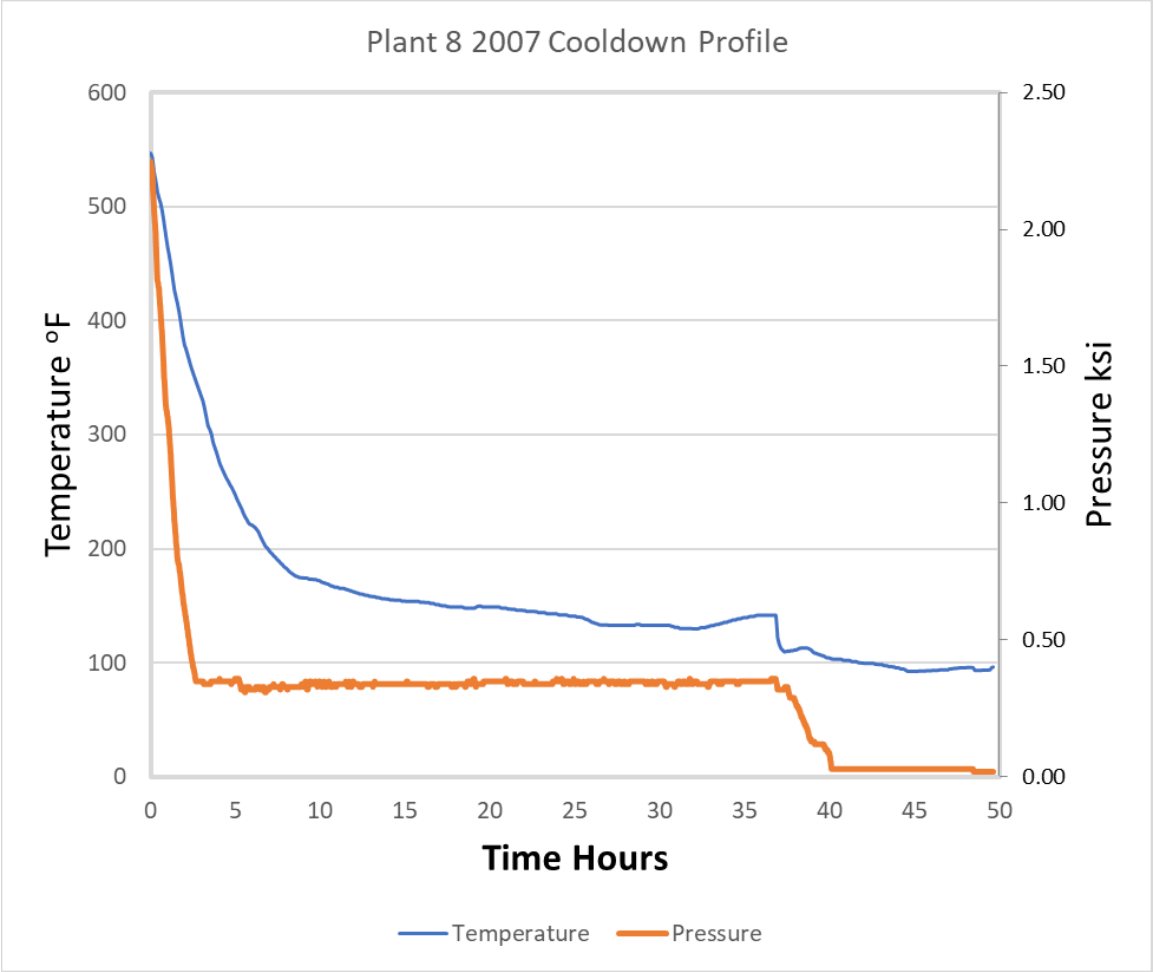

Figure 6 – Actual Plant 8-2007 Pressure-Temperature Profile

The FAVOR code was used for a deterministic calculation of applied stress for the Plant 8-2007 transient based on PWR A geometry for a 3% surface breaking flaw. The FAVOR calculated K_I for this flaw with aspect-ratios of six and infinity is shown in Figure 7. As shown in this figure, the 15-minute cooldown which occurs about 37 hours into the cooldown at a rate of about 114°F per hour produces a spike in applied stress. This spike in applied stress explains why the CPI for the Plant 8-2007 cooldown is higher than the other cooldowns shown in Figure 5. The K_{Ic} and aK_{Ic} for the Plant 8-2007 cooldown assuming the PWR A embrittlement are also shown in Figure 7.

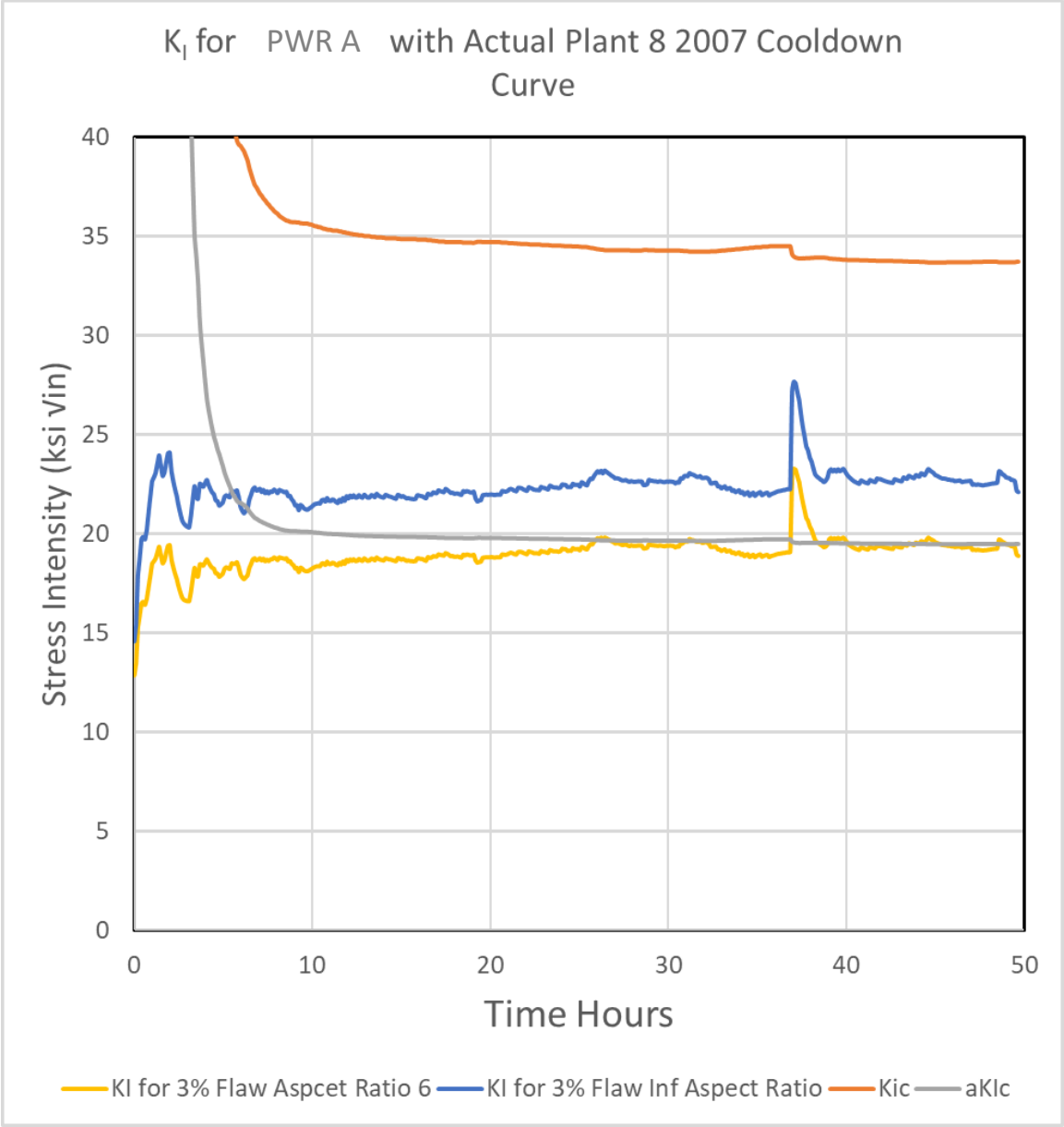

Figure 7 – Applied Stress Intensity for Plant 7-2007 Cooldown with PWR A 3% Flaw

The Plant 7-1997 cooldown transient pressure-temperature profile is shown in Figure 8. As shown in this figure, the Plant 7-1997 transient began with a 100-hour time period where the pressure remained close to the 2250 psia normal operating pressure while the temperature the RCS temperature was reduced to approximately 350°F. At 100 hours, there is a slow pressure deduction from 2200 psia to 1900 psia as the temperature is reduced from 350°F to 310°F and then a relatively rapid pressure reduction from 1900 psia to 400 psia. The Plant 7-1997 transient occurs over an approximately 10-day period and the RCS pressure is never reduced enough to allow reactor vessel head removal. Based on this pressure-temperature profile, the Plant 7-1997 transient was not related to a shut-down for refueling. It appears to have resulted from a plant issue that required the plant to go to zero power followed by a slow cooldown maintaining maximum pressure to allow a quick return to power. This

Plant 7-1997 transient was included with refueling cooldowns to broaden the range of transients considered.

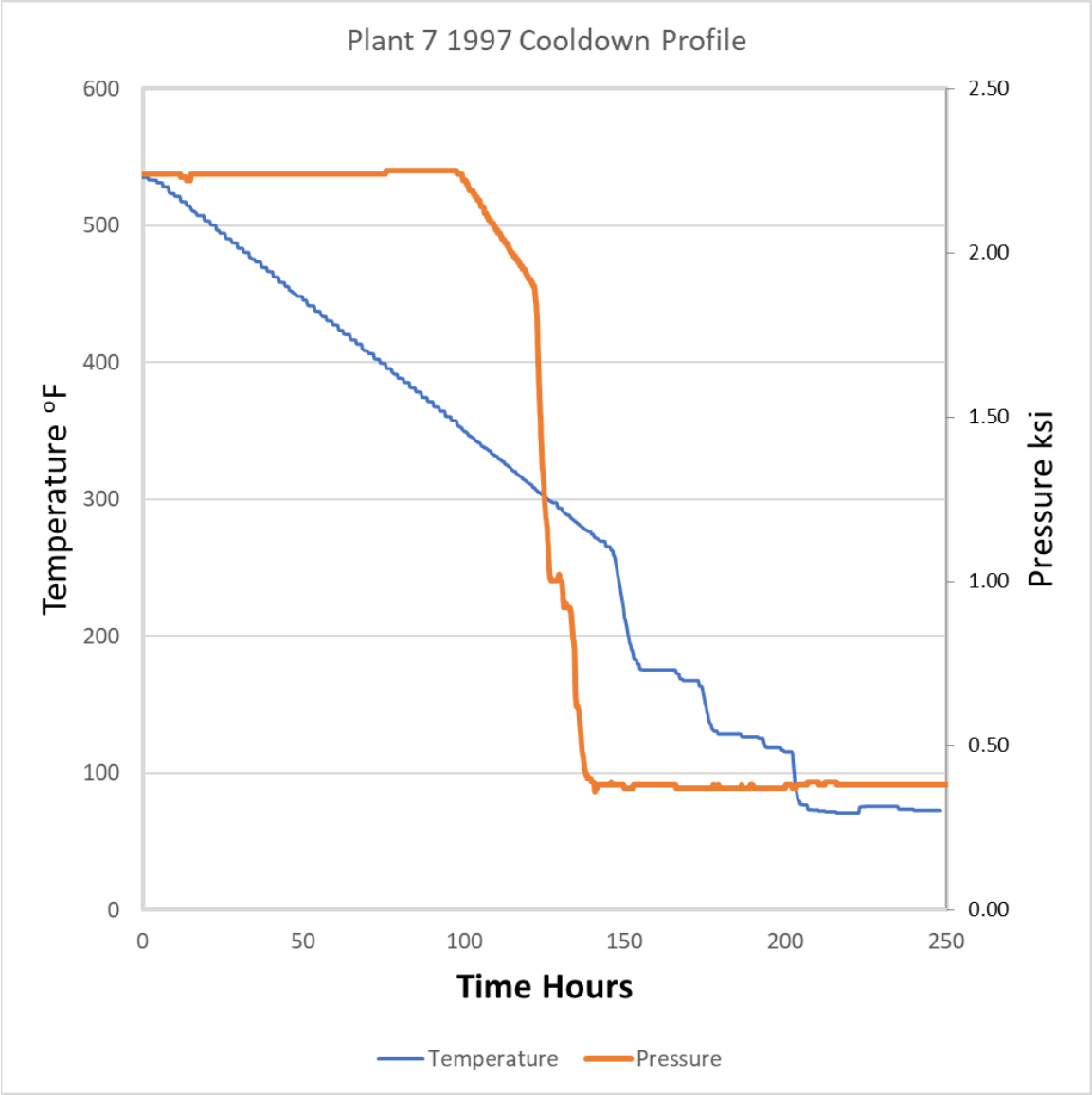

Figure 8 – Actual Plant 7-1997 Pressure-Temperature Profile

The FAVOR code was used for a deterministic calculation of applied stress for the Plant 7-1997 based on PWR A geometry for a 3% surface breaking flaw. The FAVOR calculated K_I for this flaw with aspect-ratios of six and infinity is shown in Figure 9. As shown in this figure, the cooldown at about 200 hours produces the highest applied stress of the transient. Therefore, crack initiation and propagation are not prevented for the 3% shallow flaw. The K_{Ic} and aK_{Ic} for the Plant 7-1997 cooldown assuming the PWR A embrittlement are also shown in Figure 9.

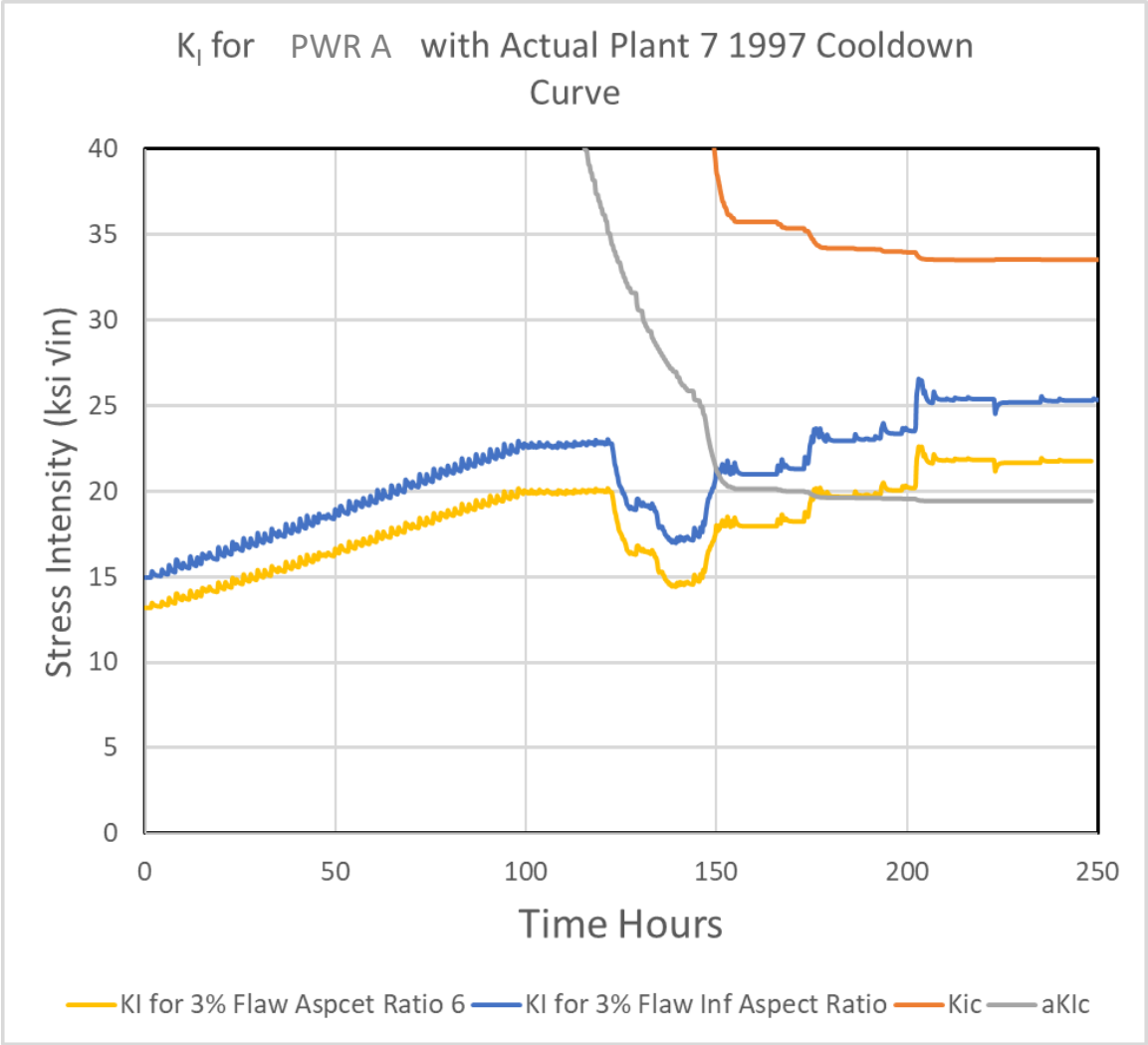

Figure 9 – Applied Stress Intensity for Plant 7-2007 Cooldown with PWR A 3% Flaw

2.3 50/30/16°F per Hour Generic Cooldown Profile

A representative pressure-temperature profile was developed based on the actual cooldowns. As shown in Figure 5, actual cooldowns exhibit a wide range of profiles. In previous evaluations, the cooldown profile selected was based on the maximum cooldown rate at the maximum pressure allowed by ASME Section XI, Appendix G. As shown in NUMARK 2018, this maximum pressure profile produces high applied stress early in the transient and tends to over-estimate the probability of warm pre-stress.

Cooldown at the maximum rate of 100°F per hour at the typical reduced pressure for refueling cooldowns results in maximum applied thermal stress at low temperature without over-estimating the potential for warm pre-stress. As shown in Figure 2, warm pre-stress still occurs for the ¼ thickness maximum flaw depth specified in ASME Section XI, Appendix G. However, as shown in Figure 3, Figure 4, Figure 7 and Figure 9, the maximum applied stress for shallow flaws for a 100°F per hour cooldown and for the actual plant cooldowns generally occurs near the end of the transient after the applied stress

exceeds aK_{Ic} and K_{Ic}. Therefore, shallow flaws are more limiting for normal plant cooldown transients than the ASME specified ¼ thickness flaw.

While an assumed cooldown at a constant rate set to the maximum 100°F per hour rate allowed by ASME Section XI, Appendix G is conservative, actual plant cooldowns as shown in Figure 5 generally show reduced cooldown rates at temperatures below about 300°F and the plants generally seem to complete the cooldown at about 100°F and atmospheric pressure in order to open the reactor vessel head. A generic profile was defined to approximate these actual cooldowns as shown by the blue line in Figure 5. This temperature represents a step wise cooldown rate of 50°F per hour for five hours from 550°F to 300°F. The cooldown continues at a rate of 30°F per hour for 5 hours from 300°F to 150°F and at 16°F per hour for 5 hours from 150°F to 70°F. This generic temperature profile is shown in Figure 10.

The FAVOR code was used for deterministic calculations of applied stress for the generic Figure 10 pressure-temperature profile. The FAVOR code was used to calculate K_I for PWR A geometry for a 3% surface breaking flaw and for PWR B geometry with a 4% surface breaking flaw. The applied stress for these PWR A (3%) and PWR B (4%) flaws with aspect-ratios of six and infinity are shown in Figure 11 and Figure 12. The FAVOR code was used for probabilistic fracture mechanics for this generic 50/30/16°F per hour cooldown for the PWR A, PWR B, PWR C and PWR D flaws shown in Table 1 and these results of these analyses are shown in Table 6.

Table 6 – Evaluation of Shallow Flaws for 50/30/16°F per Hour Cooldown

Plant Geometry	Cooldown Profile	Flaw Depth	CPI $_{mean}$	CPF $_{mean}$	Transients per year	Crack Initiation /year	TWFC
PWR A	50/30/16°F per hr	3%	4.19E-06	6.82E-09	1.00E+00	4.19E-06	6.82E-09
PWR B	50/30/16°F per hr	4%	1.20E-06	3.38E-11	1.00E+00	1.20E-06	3.38E-11
PWR C	50/30/16°F per hr	3%	5.22E-08	4.70E-10	1.00E+00	5.22E-08	4.70E-10
PWR D	50/30/16°F per hr	2%	2.64E-08	1.20E-12	1.00E+00	2.64E-08	1.20E-12

For each of the four plants evaluated in Table 6, the CPI/CPF and TWCF values for the generic 50/30/16°F are higher than all the actual 11 plant cooldowns for the same plant. Therefore, this generic 50/30/16°F is conservative compared to the 11 actual cooldown profiles. The CPI/CPF and TWCF for the 50/30/16°F per hour cooldown is significantly lower than for the 100°F per hour cooldowns shown in Table 4. The highest TWCF for the 50/30/16°F cooldown is less than 6.8×10^{-9} compared with TWCF values as high as 3.2×10^{-4} for the constant 100°F per hour constant cooldown rate.

As shown in Figure 5, actual plant cooldowns for refueling outages tend to exhibit significantly lower cooldown rates after plant cooldown switches over from heat removal with the condenser to heat removal by the RHR system. Plant RHR systems are liquid (RCS) to liquid (service water) heat exchangers that tend to have less heat removal capacity than heat removal by the normal plant condensers. As the RCS temperature approaches the service water temperature, the RHR heat removal capacity is reduced. While these factors tend to result in lower cooldown rates at lower temperatures near the lower shelf

for aK_{Ic} and K_{Ic}, licensing and Technical Specifications limits generally do not require low cooldown rates at low temperature. As shown in the Plant 8-2007 cooldown profile, high cooldown rates seem to be possible at relatively low temperature. Therefore, while reduced cooldown rates at low temperature significantly reduce the potential for shallow flaw crack initiation and propagation, these reduced cooldown rates are not required.

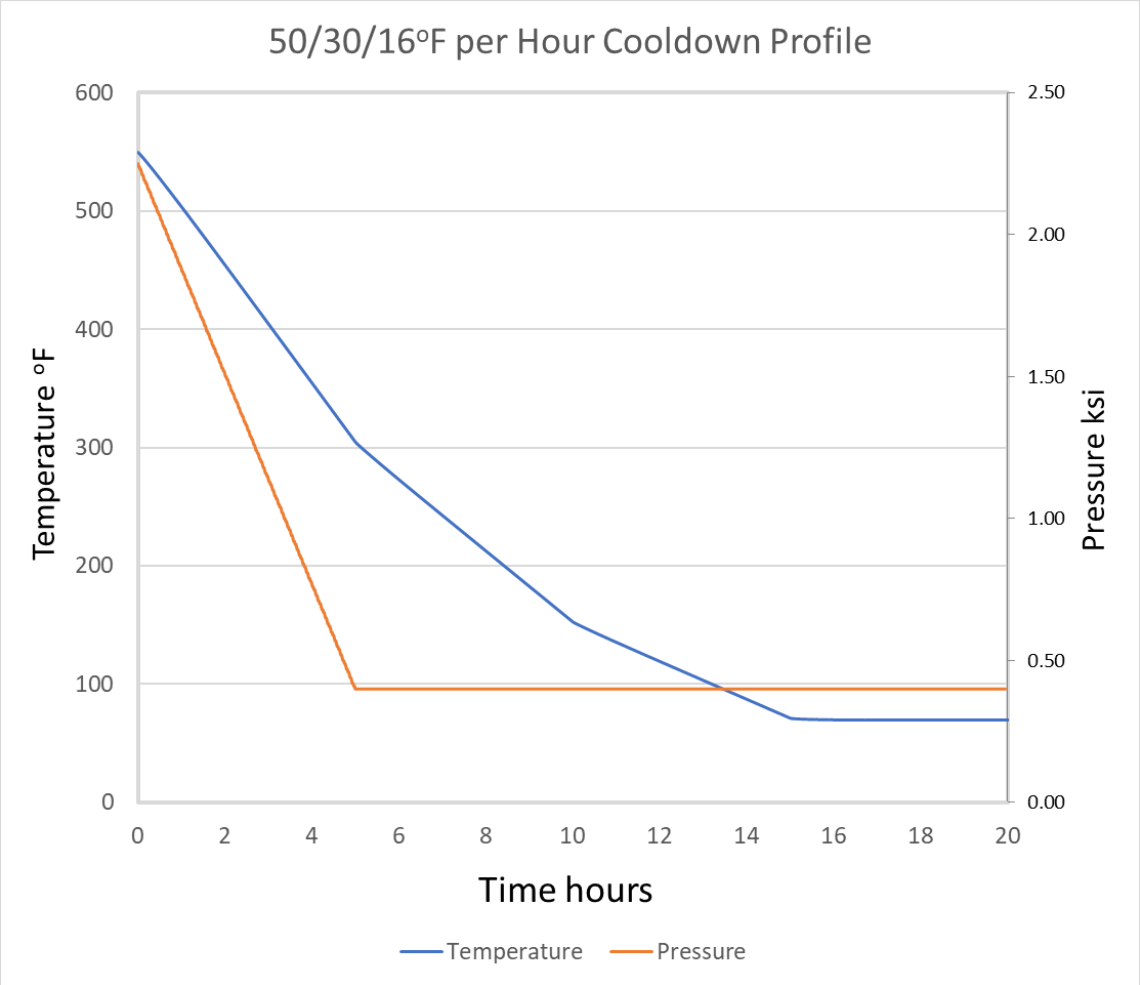

Figure 10 – Generic Pressure-Temperature Profile

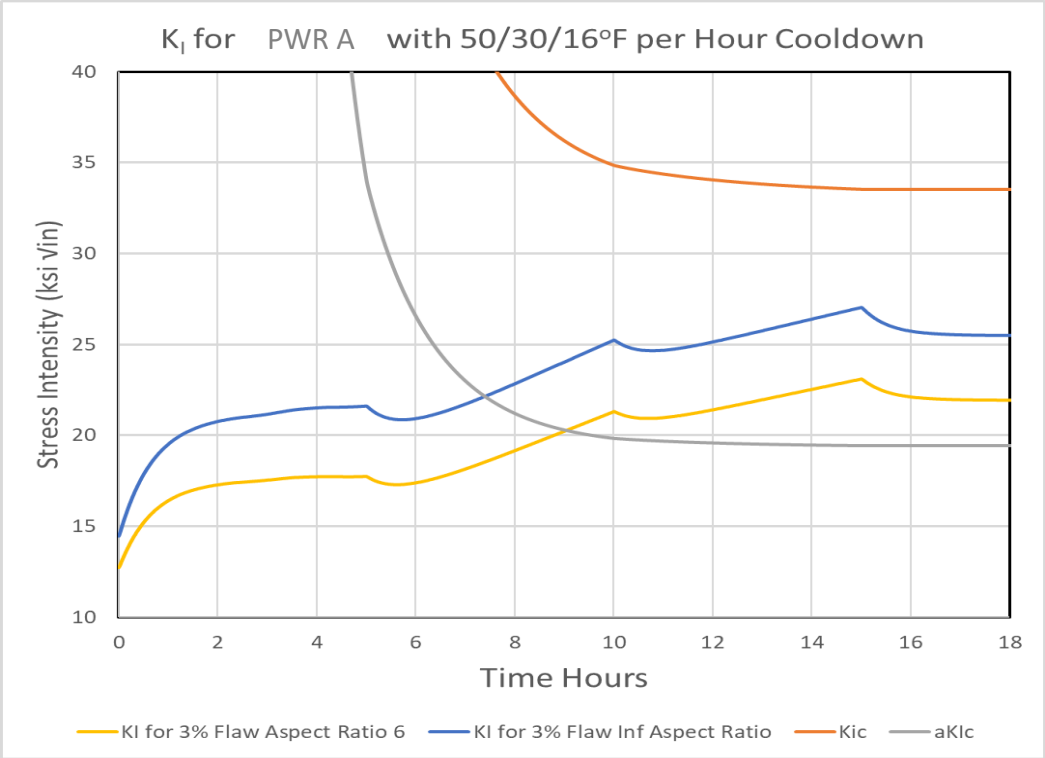

Figure 11 – Generic (50/30/16°F Cooldown) K_I for PWR A 3% Flaw

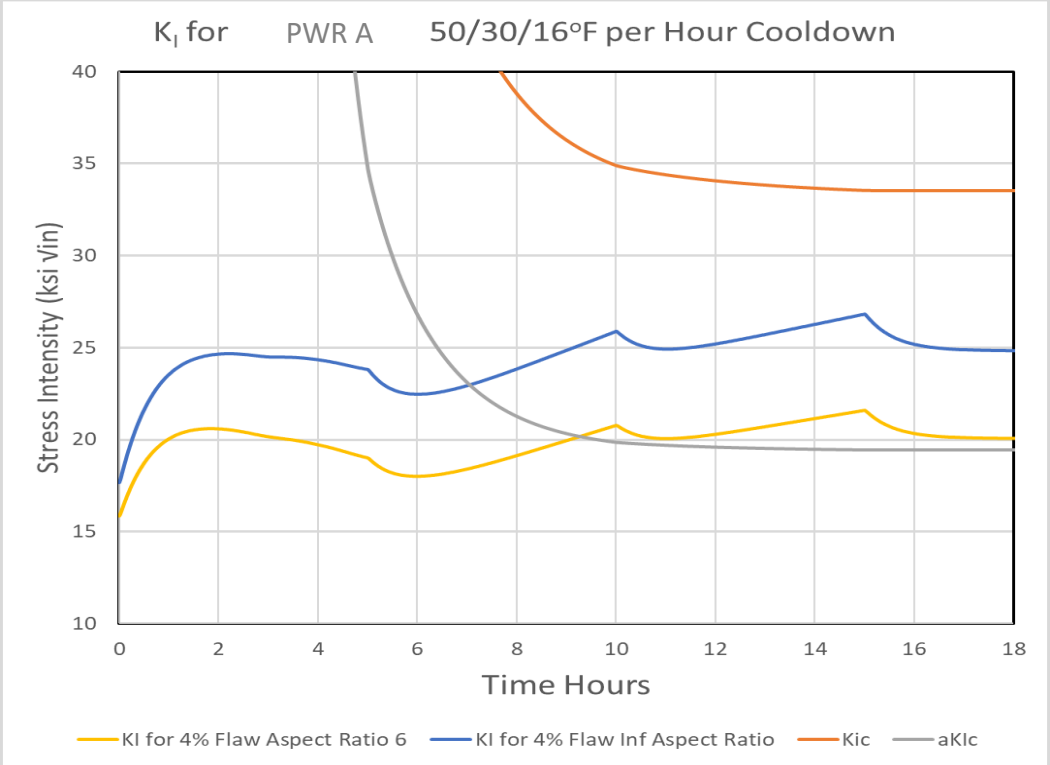

Figure 12 – Generic (50/30/16°F Cooldown) K_I for PWR B 4% Flaw

2.4 100/30/16°F per Hour Generic Cooldown Profile

As shown in Figure 5, the generic 50/30/16°F per hour cooldown profile does not bound all the actual cooldowns. A second generic cooldown profile of 100/30/16°F per hour also considered as shown in Figure 13. As shown in this figure, this 100/30/16°F cooldown profile bounds all the actual cooldown profiles.

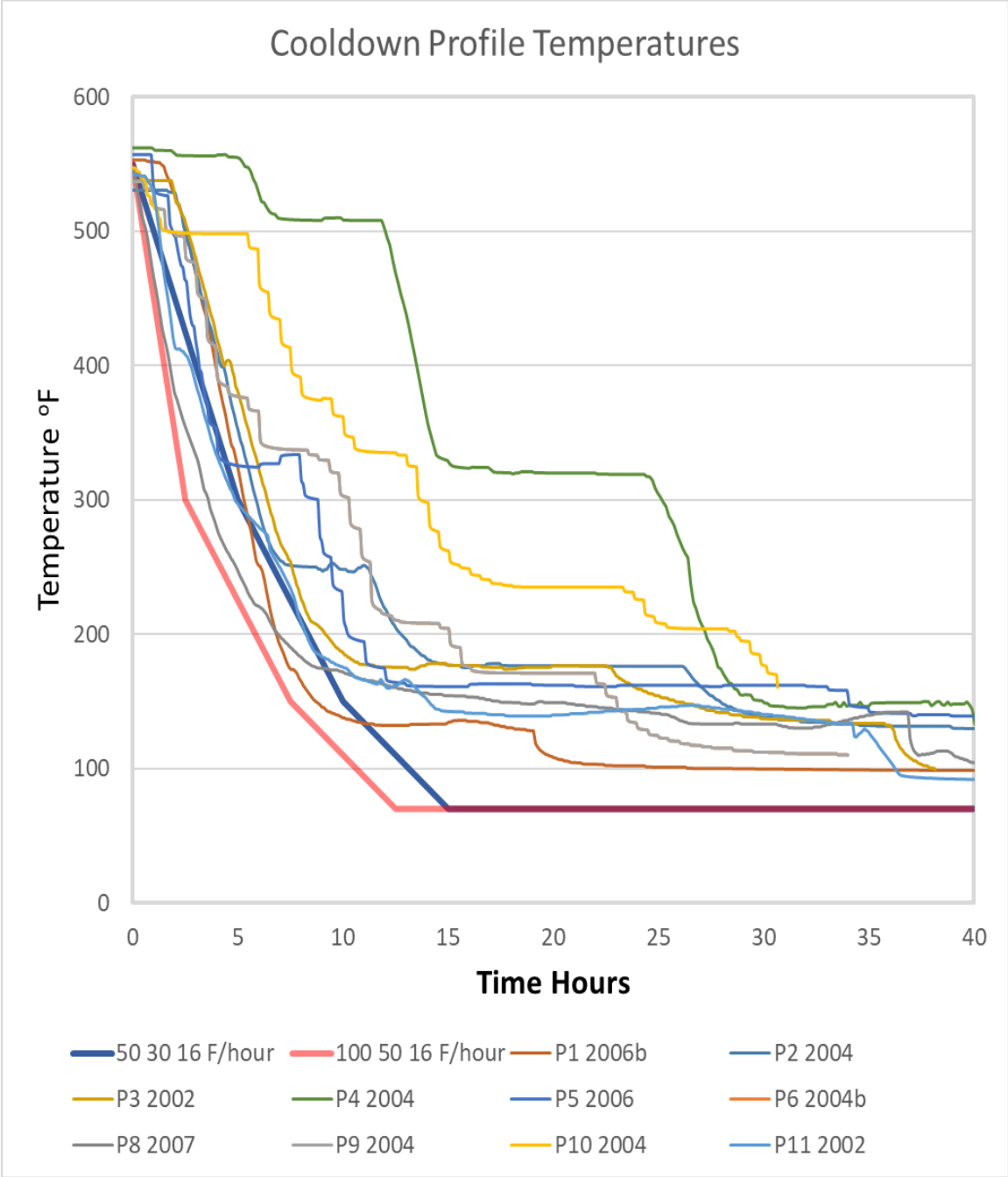

Figure 13 – 100 50 16°F per hour cooldown profile

While the 100/30/16°F cooldown profile bounds the temperature versus time of the actual plant cooldowns, this profile does not bound the CPI and CPF values for the actual cooldowns. As shown in Table 7, the TWCF for the 100/30/16°F per hour cooldown profile does not bound all the actual transients. Therefore, the more representative 50/30/16°F per hour cooldown profile was selected as the best representative and conservative generic cooldown profile.

Table 7 – Evaluation of TWCF for 100/30/16°F per hour cooldown profile

Plant Geometry	Cooldown Profile	Flaw Depth	CPI $_{mean}$	CPF $_{mean}$	Transients per year	Crack Initiation /year	TWCF
PWR A	100/30/16°F per hr	3%	6.52E-07	5.93E-10	1.00E+00	6.52E-07	5.93E-10
PWR B	100/30/16°F per hr	4%	0.00E+00	0.00E+00	1.00E+00	0.00E+00	0.00E+00
PWR C	100/30/16°F per hr	3%	2.48E-08	2.51E-10	1.00E+00	2.48E-08	2.51E-10
PWR D	100/30/16°F per hr	2%	2.64E-08	1.20E-12	1.00E+00	2.64E-08	1.20E-12

3 Impact of Coefficient of Thermal Expansion on Shallow Flaw TWCF

As shown in NUMARK 2018, FAVOR calculations of shallow flaw CPI/CPF are very sensitive to the values of Coefficient of Thermal Expansion (CTE). The higher CTE for stainless steel compared to ferritic steel is a significant factor in applied stress at low temperature for shallow flaws. As discussed in NUMARK 2018, a study by the Swedish Nuclear Power Inspectorate (SKI), Reference (5), provided an estimate of stainless steel CTE approximately 7% higher (relative) than the ASME 1998 values used in FAVOR. These higher SKI CTE values were used along with the Figure 10 (50/30/16°F per hour) cooldown profile to perform FAVOR analyses of the same plants shown in Table 6. This rather small 7% relative increase in CTE increases the calculated TWCF from a range of 10^{-12} to 10^{-9} shown in Table 6 to a range of 10^{-7} to 10^{-5} as shown in Table 8. This analysis illustrates the importance of CTE for shallow flaw evaluation.

Table 8 – Evaluation of Shallow Flaws for 50/30/16°F per hour Cooldown Profile with SKI CTE

Plant Geometry	Actual Cooldown	Flaw Depth	CPI $_{mean}$	CPF $_{mean}$	Transients per year	Crack Initiation /year	TWFC
PWR A SKI CTE	50/30/16°F per hr	3%	3.45E-04	8.82E-05	1.00E+00	3.45E-04	8.82E-05
PWR B SKI CTE	50/30/16°F per hr	4%	2.22E-05	8.72E-07	1.00E+00	2.22E-05	8.72E-07
PWR C SKI CTE	50/30/16°F per hr	3%	5.96E-06	1.82E-07	1.00E+00	5.96E-06	1.82E-07
PWR D SKI CTE	50/30/16°F per hr	2%	3.68E-05	1.02E-05	1.00E+00	3.68E-05	1.02E-05

4 Summary and Recommendations

FAVOR analyses were performed of shallow internal surface-breaking flaws based on the assumption of one flaw per vessel that extends just into the ferritic steel (as shown in Table 1) and a constant cooldown from operating temperature to ambient at 100°F per hour. As shown in Table 4, expected TWCF values in the range of 10^{-6} for a low embrittlement plant (PWR D at 60 EFPY) to 10^{-4} for a higher embrittlement plant (PWR A at 60 EFPY) were obtained.

To compare ASME Section XI, Appendix G maximum cooldown rate of 100°F per hour TWCF calculations with actual cooldowns, one actual cooldown profile was selected from 11 different PWR plants. The FAVOR-calculated TWCF for these 11 cooldown profiles using the PWR A plant geometry and embrittlement (60 EFPY) is shown in Table 5. The TWCF values for these actual cooldown profiles range from zero up to 10^{-8} – several orders of magnitude lower for the actual cooldowns compared with cooldown to ambient at a constant rate of 100°F per hour. The other three plants (PWR B, PWR C and PWR D) with lower embrittlement were also evaluated and the TWCF values for these plants are all lower than PWR A.

In order to define a single cooldown profile similar to these actual profiles, a step-down cooldown (50°F per hour, 30°F per hour and 16°F per hour) was defined as shown in Figure 10. The FAVOR calculated TWCF for this step-down cooldown was compared with the 11 actual plant cooldowns and found to be conservative – see Table 6. As shown in this table, the FAVOR-calculated TWCF for all four plants evaluated is less than 10^{-6}.

While actual plant cooldowns seem to generally show very slow cooldown rates as the RCS temperature approaches ambient (70°F), there is no general mandate for this slow cooldown rate. The relatively slow cooldown rate for actual plant cooldowns (see Figure 5) may be the result of common practice and may also be related to the performance of plant Residual Heat Removal (RHR) systems that rely on heat exchangers. The RHR systems tend to become less effective as the RCS temperature approaches the plant service water temperature. Regardless of the reason why the actual plant cooldowns show reduced cooldown rate at low temperature, this lower cooldown rate results in a significant reduction in calculated TWCF for shallow flaws. The lower cooldown rate for actual plant transients generally seems to reduce the shallow flaw TWCF to less than 10^{-6} assuming one single shallow surface breaking flaw per plant and one cooldown transient per year. **As a result, further study is recommended to see whether a generic temperature profile like the one in Figure 10 can be assumed for future shallow flaw analysis instead of the 100°F per hour maximum cooldown rate based on ASME Section XI, Appendix G.**

The results of this study suggest that the assumption in ASME Section XI, Appendix G that cooldown transients and maximum cooldown rate and pressure should be based on a ¼ thickness flaw is not conservative. A ¼ thickness flaw will generally be prevented from crack initiation and propagation by warm pre-stress well before the vessel flaw temperature approaches K_{IC} or aK_{Ic}. Evaluations of cooldown transients should consider shallow flaws that may not be protected from crack initiation by warm pre-stress. The applied stress for these shallow flaws at low temperature will be less than the applied stress for a ¼ thickness flaw. However, these shallow flaws are generally not protected by warm pre-stress like the ¼ thickness flaw.

As shown by the analyses in Section 3, FAVOR shallow flaw **TWCF is very sensitive to the difference between the CTE of the stainless steel and ferritic steel**. A small percentage change in CTE can result in

changes of TWCF by orders of magnitude. Because of this sensitivity, **further study of stainless steel and ferritic steel CTE is recommended**.

Another recommended area for future evaluation concerns small underclad flaws. Shallow surface breaking flaws are considered very unlikely to occur because these flaws would have to be created during the application of the stainless-steel cladding and extend into the ferritic steel. However, another type of flaw that could occur is a flaw in the surface of the ferritic steel that could be created during RPV fabrication. This type of small underclad flaw may be subject to stress from differential thermal expansion between the stainless-steel and ferritic steel just like the small extension of shallow surface breaking flaw that extends just into the ferritic steel. **Further study of underclad flaws is recommended.**

5 References

1. **Bass, Richard B, et al.** *The Effect of Shallow Inside-Surface-Breaking Flaws on the Probability of Brittle Fracture of Reactors Subjected to Postulated and Actual Operational Cool- Down Transients: A Status Report.* s.l. : ORNL/TM-2015/59531/Rev-01, 2016.
2. **NUMARK.** *Assessment of Reactor Pressure Vessel Inside Diameter Shallow Surface Breaking Flaws.* 2018.
3. *A Computer Code for Fracture Mechanics Analysis of Nuclear Reactor Pressure Vessels, PVP 2017-65262.* **Bass, Richard B, et al.** Waikoloa, Hawaii : Procedings of the ASME 2017 Pressure Vessels and Piping Conference, July 16-20, 2017.
4. **ASME.** *ASME Boiler and Pressure Vessel Code, Section XI, Appendix G.* New York : s.n., 2004.
5. **Iradj, Sattri-Far and Anderson Magnus.** *Cladding Effects on Structural Integrity of Nuclear Components.* s.l. : Swedish Nuclear Power Inspectorate (SKI), June 2016.
6. **Williams, P.T., et al.** *Fracture Analysis of Vessels – Oak Ridge FAVOR, v16.1, Computer Code: Theory and Implementation of Algorithms, Methods, and Correlations, ORNL/LTR-2016/309.* s.l. : Oak Ridge National Laboratory, Spetember 2016.

6 Appendix A – Discussion of Flaw Depth

As discussed in Reference (1), the maximum CPI for shallow flaws generally occurs at the flaw depth that is just beyond the clad thickness. Because FAVOR only allows specifying flaw depths in 1% increments, the analyses below start at the 1% flaw depth increment just beyond the clad thickness and then increase by 1% until the flaw depth extends beyond the thickness impacted significantly by the difference between stainless steel clad and ferritic vessel steel coefficient of thermal expansion (CTE). As shown in Figure 14, the impact of stresses from differential CTE causes high CPI values that extend over approximately a 1% depth of the vessel wall thickness. At greater flaw depth CPI drops by several orders of magnitude.

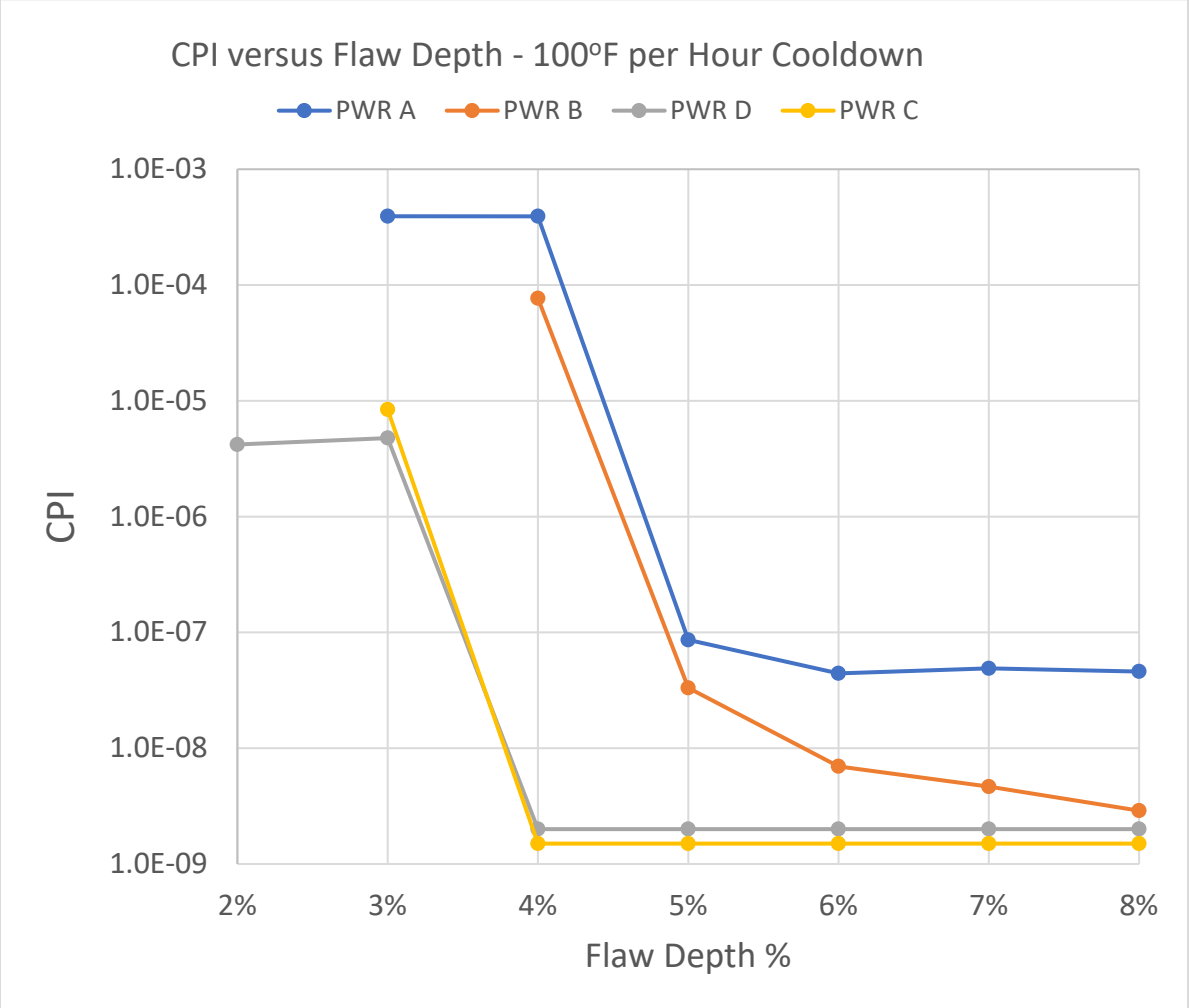

Figure 14 – CPI versus Flaw Depth for 100°F per Hour Cooldown

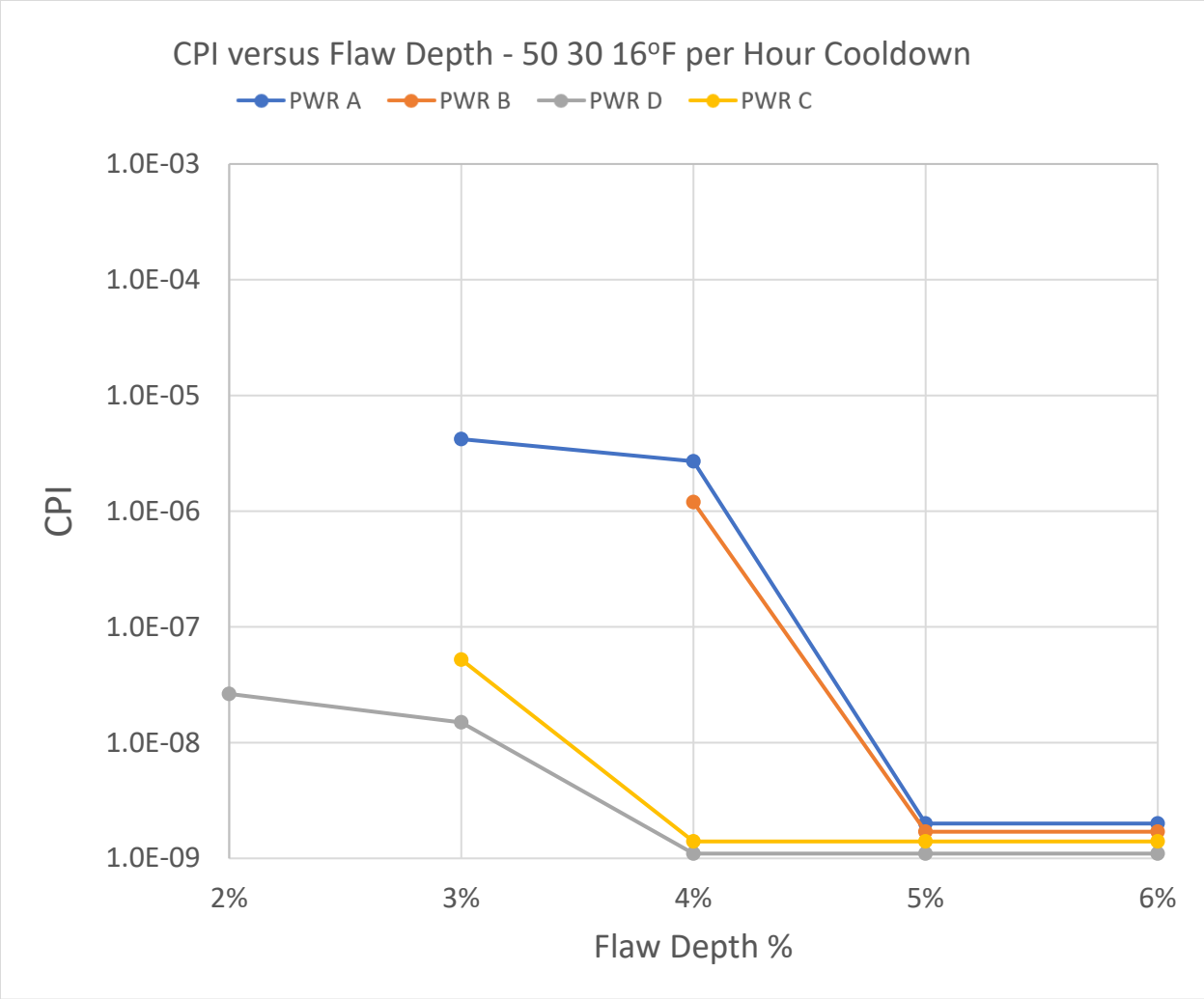

Figure 15 – CPI versus Flaw Depth for 50/30/16ºF per Hour Cooldown